Adsorption of CO_2 by synthetic zeolites

Francesco Ferella[1,*], *Valentina* Innocenzi[1], *Nicolò M.* Ippolito[1], and *Ida* De Michelis[1]

University of L'Aquila, Department of Industrial and Information Engineering and Economics, 67100 L'Aquila, Italy

Abstract. The paper reports on a possible way to recycle fluid catalytic cracking catalysts (FCCCs), widely used in oil refining operations. This research proposes a novel approach that leads to a near zero-waste process. The spent FCCC was leached by 1.5 mol/L of HNO_3, HCl and H_2SO_4 solutions at 80°C, for 3 h with a solid to liquid ratio of 20 %wt/vol. The leaching yields for cerium and lanthanum were in the range 69-82 %. The solid residues from the leaching stage were used as base material for the synthesis of the zeolites by means of a combined thermal-hydrothermal treatment. The characterization of the zeolites demonstrated that the Na-A phase was predominant over the Na-X phase. The zeolites were tested as sorbent material for CO_2 separation from CH_4, in order to simulate the upgrading of biogas to biomethane. The maximum adsorption rate of CO_2 was 0.778 mol CO_2/kg of zeolite at 3 bar, with a resulting CH_4 recovery of 62 % and purity of 97 %vol. The zeolites synthesized from spent FCCC represent a feasible solution to recover such industrial waste.

1 Introduction

FCC plays a crucial role in conversion of heavy fractions into lighter ones like naphtha, and thus it is one of the most important catalytic process in the oil refining industry. Open landfills and the temporary storage sites have been the main choice to manage such waste for many years. The FCC catalysts contain about 3-3.5 %wt. of rare earth (RE) oxides, in particular lanthanum (La) and cerium (Ce) that enhance the catalytic activity and act as a "bridge" to stabilize aluminium atoms in the carrier. The recovery of REs from spent FCCCs was never tried so far at a big scale, as their concentration is too low for the profitability of the investment.

Wang et al. [1] recovered La and Ce from FCC waste slag by leaching with HCl and selective precipitation of the REEs as $NaRE(SO_4)_2 \cdot xH_2O$. Wang et al. [2] leached FCC waste slag by a NaOH solution in order to convert Al into soluble $NaAlO_2$, that can be used further as secondary raw material. The total recovery of La and Ce was 97.6 %. The most used technique for the extraction of REEs from leach liquors is solvent extraction: 2-ethylhexyl phosphoric acid-2-ethylhexyl ester (EHEHPA) in kerosene was used to recover La and Ce previously leached from spent FCCC by HCl. The yields for the leaching, extraction and stripping stages were 85, 100 and 96 %, respectively [3].

Innocenzi et al. [4] also applied solvent extraction by di-(2-ethylhexyl) phosphoric acid (D2EHPA) of Ce and La from hydrochloric pregnant solutions: the overall REEs recovery was 62.9 % [5]. HCl and chlorine are among the most effective leachants in the treatment of ores and materials containing metals [6]. Ion-exchange is a suitable technique to extract REEs from leach liquors [7], for instance by polyacrylate anion-exchanger resin (Amberlite IRA 958) [8], chemically modified Amberlite XAD-4 [9], as well as resins containing mixed sulfonic/phosphonic, amino-phosphonic or iminodiacetic acid functional groups [10]. Bioleaching is an environmentally-friendly technique whose results are still scant: the maximum REE leaching yield was 49%, achieved by *Gluconobacter oxydans*, that mainly synthesizes gluconic acid [11].

In the last years, the author of the present paper tested the CO_2 adsorption capacity of the zeolites derived from fly ash [12] and the profitability of the plant was also assessed [13]. Regarding FCCC as base material, few studies deal with zeolite synthesis and characterization only, without further applications. Only one paper investigated the Cr^{3+} adsorption onto zeolites, mixed with cement mortars containing a fraction lower than 5 % of such solid [14]. Basaldella et al. [15] tried to grind the spent FCCC before the hydrothermal treatment with NaOH solution. In that work, calcination at high temperature was not carried out and the zeolites obtained in this way were fully characterized. Liu et al. [16] synthesized zeolite Y with different particle sizes by means of FCCC fine powder. The results demonstrated that the cracking activity for heavy oil and resistance to coking of the fine zeolite catalysts were enhanced. Basaldella et al. [17] tested alkaline fusion with different FCCC/Na_2CO_3 ratios at 800°C for 2 h, followed by hydrothermal crystallization with 4 mol/L NaOH solution at 80°C in presence of $NaAlO_2$. Conversion to Na-A (LTA) zeolite greater than 50% was obtained in all the crystallization tests.

* Corresponding author: francesco.ferella@univaq.it

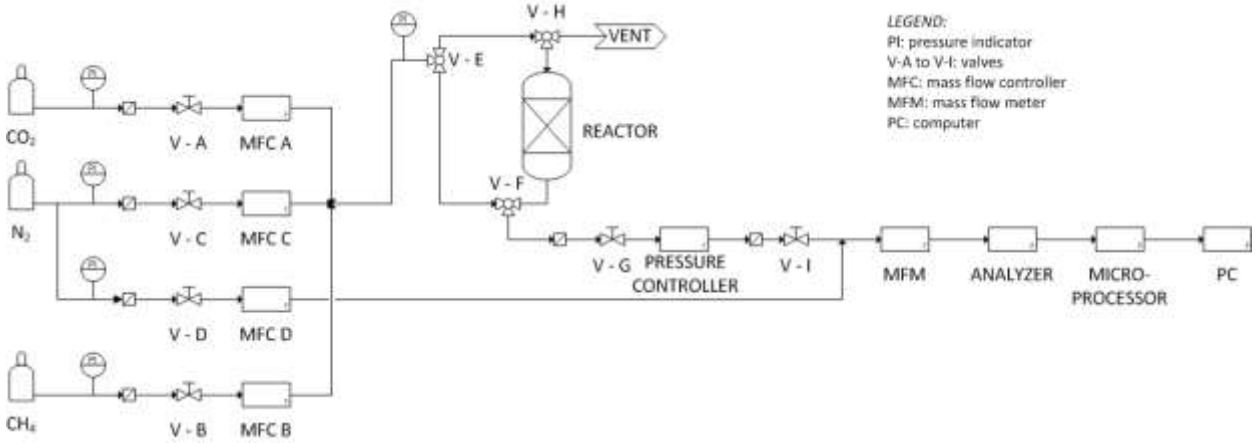

Fig. 1. Process flow diagram of the lab-scale plant.

2 Materials and Methods

2.1 Characterization of spent FCCC

The spent FCCC was supplied by Orim S.p.a. (Macerata, Italy). The sample was characterized in terms of metal content by X-ray fluorescence (XRF) (Spectro, Xepos) and inductively coupled plasma (ICP-OES, 5110 Agilent Technologies), X-ray diffraction (XRD, PANalytical X'Pert PRO), particle size distribution (PSD, Mastersizer 2000, Malvern), Brunauer-Emmet-Teller (BET) specific surface area (SSA, NOVA 1200e, Quantachrome porosimeter) and scanning electron microscopy (SEM) (20 kV Philips XL30 CP microscope).

2.2 Leaching tests

Three different inorganic acids were investigated: HCl, HNO_3 and H_2SO_4 at a constant concentration of 1.5 mol/L and fixed the solid to liquid (S/L) ratio equal to 200 g/L. The temperature was kept constant at 80°C for 3 h. The detailed experimental procedure is detailed in [12]. The tests for the recovery of La and Ce from the pregnant solutions were not reported here. The solids resulting from the filtrations were stored for the following production of zeolites.

2.3 Production and characterization of zeolites

The synthesis procedure was similar to that used with fly ash in a previous work [12]: two stages of the procedure were changed, in particular the thermal treatment that was carried out at 750°C for 1.5 h, and the hydrothermal activation, that lasted 12 h at 95°C. The zeolites were characterized as for spent FCCC (see paragraph 2.1). The zeolites were thus used to test their capacity in the adsorption of CO_2 from a CO_2/CH_4 gas mixture, simulating a typical biogas composition.

2.4 CO_2 adsorption tests

Continuous dynamic trials were carried out in order to evaluate the sorption capacity of the three synthetic zeolites under typical industrial conditions. The arrangement of the lab-scale apparatus used for the tests is shown in Fig. 1.

The apparatus was already described in detail, as well as the experimental procedure adopted [12]. CH_4 and CO_2 were injected in the reactor in a ratio equal to 53/47 %vol., in order to simulate a real biogas mixture. One first-order and dead time mathematical model was proposed to determine the amount of the adsorbed CO_2 [18]. During the adsorption phase, the total CH_4 recovery can be computed directly as:

$$CH_4^{out} = CH_4^{in} - CH_4^{ads} \quad (1)$$

Hence, knowing the total amount of CH_4^{in} injected (mol, measured before the test) and the amount that left the reactor (CH_4^{out} directly measured), it is possible to calculate the CH_4^{ads} adsorbed onto the zeolites, that shall be close to zero. The purity of CH_4 can be computed as:

$$CH_4^{pur} = \frac{CH_4^{out}}{CH_4^{out} + \left(CO_2^{in} - CO_2^{ads}\right)} \quad (2)$$

The difference CO_2^{in}-CO_2^{ads} (mol) is the amount of CO_2 not adsorbed, and that thus contaminates the CH_4 recovered. On the other hand, the total CO_2 recovery can be calculated as:

$$CO_2^{ads} = CO_2^{in} - CO_2^{out} \quad (3)$$

whereas, the purity can be estimated as:

$$CO_2^{pur} = \frac{CO_2^{ads}}{CO_2^{ads} + CH_4^{ads}} \quad (4)$$

Table 1. XRF analysis of the spent FCCC.

	Concentration (%wt)									
Sample	Na	Al	Si	P	Ti	V	Fe	Ni	La	Ce
FCCC	-	15.60	12.30	0.13	0.47	0.050	0.25	0.03	2.30	0.16

In the ideal conditions, CH_4^{ads} is zero, so that the CO_2 purity is 1. This is very important as CO_2 can be a valuable by-product of the biogas separation plant, that could be liquefied and sold for many industrial purposes like beverage, fire extinguishers, metal inert gas welding, refrigeration. When using the four formulas (1)-(4), the CH_4^{pur} was fixed to 97%, as the minimum value provided for by the Italian law for injection in the distribution grid is 95%. Hence, the other three key parameters were calculated accordingly.

3 Results and Discussion

3.1 Characterization of spent FCCC

The concentration of the main elements is listed in Table 1.

Ce and La, as well as Al and Si, that represent the most concentrated elements in FCCC and are dissolved in great amount during leaching, were also measured by ICP-OES. The latter analysis gave the following values: Al 31.75 %, Si 19.46 %, La 1.57 %, Ce 0.19 %wt. The main crystalline phase found in the FCCC sample was dealuminated zeolite Na-Y; the other minor phases were zeolite ZSM-5 and alumina (see Fig. 2). The particle size distribution was represented by a Gaussian curve centered at 80.4 μm, that is the D_{50}, whereas the Sauter's diameter D[3,2] was 73.6 μm. Regarding the BET analysis, the SSA was nearly 112 m^2/g, not so lower than the SSA of a fresh FCCC, that is usually in the range 120-180 m^2/g [19].

3.2 Leaching tests

The extraction yields obtained at different reaction times are listed in Table 2. As it can be inferred from the results, the extraction of Ce and La with the HNO_3 solution is lower than the corresponding extractions achieved with HCl and H_2SO_4. In the latter case, at 3 h, the average extraction yields for Ce and La are around 73 % and 81 %, respectively. Hence, increasing the reaction time by one hour, the extraction yields of La and Ce, the most important metals we are interested in, do not enhance significantly, so that 2 h can be selected as optimum reaction time. The extraction of Si and Al are very similar in all the leaching tests, nearly 1.1 % and 20 %, that correspond to around 200 mg/L and 11.5 g/L, respectively. Unfortunately, such concentrations of Si and Al entail many problems in the following recovery stage for Ce and La [19] (here not discussed).

Table 2. Extraction yields in the leaching tests.

	Extraction yield (%)			
Sample	Ce	La	Si	Al
HNO_3 2h	67.9±1.6	76.6±2.1	1.1±0.1	18.4±0.4
HNO_3 3h	69.6±2.5	78.8±2.6	0.9±0.1	19.4±0.6
HCl 2h	73.3±3.0	81.5±3.2	1.0±0.2	21.4±2.2
HCl 3h	72.6±3.1	80.4±3.3	0.6±0.2	20.6±2.7
H_2SO_4 2h	72.9±2.5	80.4±1.8	1.2±0.1	19.8±2.1
H_2SO_4 3h	73.3±2.2	82.1±1.5	1.4±0.2	22.7±2.3

3.3 Characterization of zeolites

The XRF composition of the three zeolites is listed in Table 3.

The Si/Al ratio is always around 1, and this confirms that these are low silica synthetic zeolites. The XRD spectra of the FCCC and zeolites are shown in Fig. 2. The HNO_3 zeolite is composed of one main phase, that is hydrated zeolite Na-A with formula $Na_{12}Al_{12}Si_{12}O_{48}\cdot 27H_2O$ in concentration of 92 %, according to the Reference Intensity Ratio (RIR) method, plus 8 % of Cl-free sodalite ($Na_8Al_6Si_6O_{24}$), another aluminosilicate mineral. Instead, the HCl zeolite is clearly composed of three phases: the same zeolite Na-A ($Na_{12}Al_{12}Si_{12}O_{48}\cdot 27H_2O$), Cl-free sodalite plus a third phase, that resulted to be dehydrated zeolite Na-X, with formula $Na_{92}Al_{92}Si_{100}O_{384}$. Zeolite Na-X is an ensemble of sodalite cages or β-cages joined by hexagonal prisms [20]. H_2SO_4 zeolite also showed the same Na-A, Na-X and sodalite phases as for the sample coming from the HCl leaching residue.

SEM pictures of the zeolites are shown in Fig. 3. Cubic crystals belong to the typical crystalline structure of zeolite Na-A. In Fig. 3a, it can be recognized the growth of the Na-A crystals on one particle of the FCCC, whereas in Fig. 3b the crystallization process for zeolite Na-A achieved a higher grade. The morphology of Na-X crystals is in the form of octahedrons, composed of eight equilateral triangles, that can be seen in Fig. 3c, where there is a mixture of Na-A and Na-X phases, the

Table 3. XRF analysis of the synthetic zeolites.

	Concentration (%wt)								
Sample	Na	Al	Si	Ti	V	Fe	Ni	La	Ce
Z-HNO_3	8.06	12.07	12.19	0.44	0.004	0.19	0.03	0.33	0.02
Z-HCl	8.24	11.93	12.27	0.45	0.005	0.20	0.03	0.35	0.03
Z-H_2SO_4	7.98	11.59	11.74	0.45	0.005	0.19	0.03	0.33	0.03

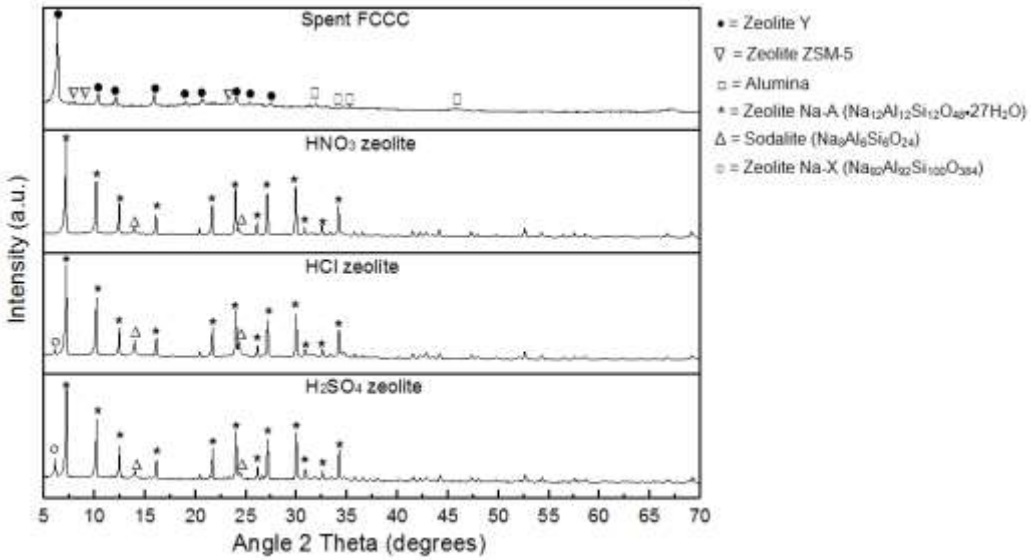

Fig. 2. XRD patterns of the spent FCC and zeolites.

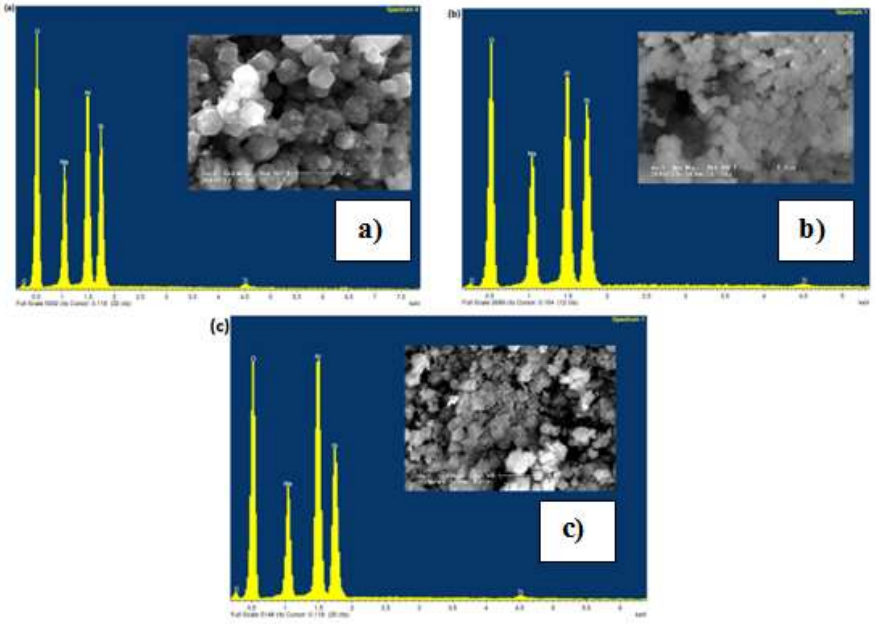

Fig. 3 SEM pictures and microanalyses of Z-HCl (a), Z-HNO_3 (b) and Z-H_2SO_4 (c).

latter present in lower concentration.

The SSA for HNO_3, HCl and H_2SO_4 zeolite samples was around 12, 26 and 83 m^2/g, respectively.

3.4 Adsorption of CO_2

The performance of the three zeolites are shown in Fig. 4, where the results are reported in terms of recovery and purity of CO_2 and CH_4, the latter being the most valuable product.

As it can be inferred from the graphs, the best results were obtained with HNO_3 zeolite at 3 bar: keeping fixed the CH_4 purity at 97 %vol., the maximum recovery of CH_4 that can be achieved is only 62 % of the total mass flowing through the reactor. This is due to the adsorption of part of CH_4 onto the zeolite, that thus is not very selective to CO_2. Such adsorbed CH_4 is released during the regeneration of the bed, when the system is depressurized to ambient pressure and the CO_2 is stripped off from the zeolite: although the recovery of CO_2 is almost quantitative, the purity is rather low, around 72 %. Regarding the specific adsorption rates, the experimental values are reported in Table 4.

Table 4 also lists the selectivity of the zeolites to CO_2, calculated by Eq. (5):

$$Selectivity = \frac{mol\,CO_2}{mol\,CH_4}, \qquad (5)$$

Table 4. Adsorption rate and selectivity of the zeolites.

	Adsorption rate (mol CO_2/kg zeolite)					**Selectivity**			
	3 bar	4 bar	5 bar	6 bar		3 bar	4 bar	5 bar	6 bar
Z-HNO_3	0.778	0.612	0.555	0.596		2.55	2.51	1.82	2.07
Z-HCl	0.271	0.276	0.315	0.367		0.55	0.72	0.75	0.75
Z-H_2SO_4	0.290	0.289	0.327	0.398		0.68	0.81	0.93	1.04

where the moles of the two gases are those adsorbed on the sorbent, so that the greater the selectivity, the better the zeolite is for biogas upgrading. It is clear that the highest selectivity is achieved by HNO_3 zeolite at 2 and 3 bar, when the lowest amount of CH_4 was adsorbed.

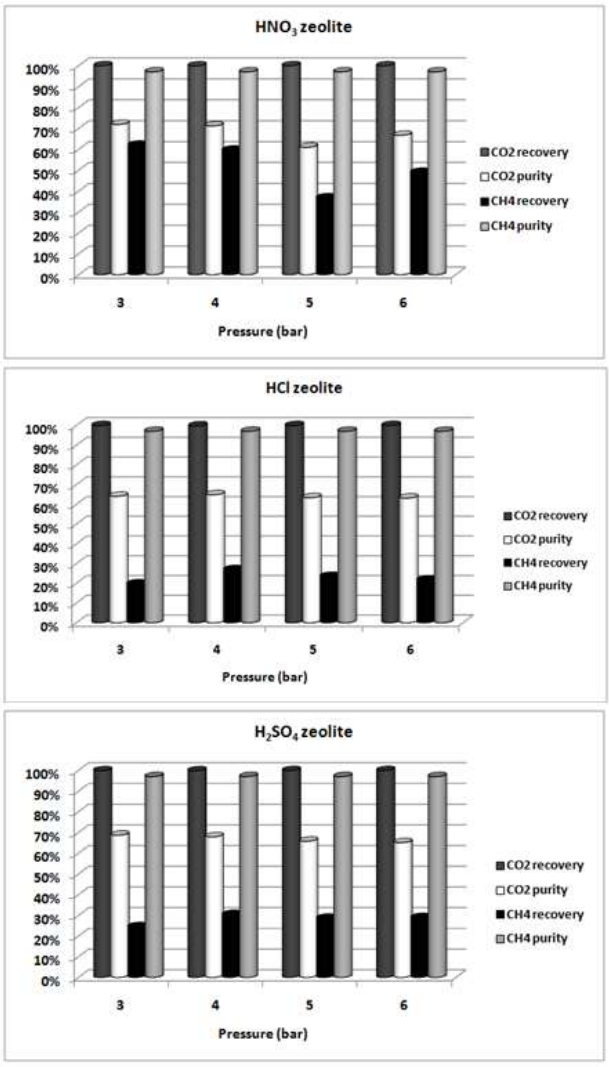

Fig. 4. Yields and grades of CO_2 and CH_4 after separation.

The best performance was achieved by the HNO_3 zeolite at 3 bar, with 0.778 mol CO_2/kg zeolite that correspond to 34.2 g CO_2/kg zeolite. This is by far the greatest value achieved in the experimental tests. The specific adsorption rate decreased with pressure with the HNO_3 zeolite, whereas it increased with pressure with the other two samples (HCl and H_2SO_4 zeolites). Nevertheless, with the last two samples, the adsorption rate was lower than that achieved with HNO_3 zeolite for each pressure value. The different trend in adsorption of the CO_2 molecule cannot be directly attributed to the SSA, as such parameter was the lowest in the HNO_3 zeolite (12 m^2/g versus 26 and 83 m^2/g for HCl and H_2SO_4 zeolite, respectively). The main difference among samples lies in the crystalline structure, that is similar for HCl and H_2SO_4 zeolites (Na-A, Na-X and sodalite), whereas the Na-X phase is missing in the structure of the HNO_3 zeolite.

Thus, what can be inferred from the cross checking of the data is that the Na-A phase is able to capture CO2 molecules more selectively over the CH4 ones: in fact, with the other two zeolite samples, the recovery of CO2 is always quantitative, but its purity is a bit lower: hence, it might also be possible that the pore distribution is centered on micropores in case of Z-HNO3, that acts as a molecular sieve for CO2 and CH4 molecules. The kinetic diameter of CH4 and CO2 is 0.376 and 0.330 nm, respectively.

The tests were conducted at ambient temperature, but the selectivity increases with the temperature. The selectivity of the HNO3 zeolite was in line with that predicted at those temperature and pressure levels by [22], although they tested a commercial zeolite 5A under equilibrium conditions. Comparing these results to those from fly ash zeolites obtained with a similar hydrothermal procedure, the main difference lies in the amount and grade of CH4 obtained, as the selectivity was 2-4 times higher; correspondingly, also the grade and the recovery of CO2 were higher than 98 %.

4 Conclusions

The sole recovery of Ce and La from spent FCCC is not profitable because of their low concentration, so that a recycling process has to be coupled with the reuse and valorization of the solid residue of the leaching stage. The most useful way is the production of zeolites, that have a wide range of industrial applications. In this paper, FCC catalyst was leached by 1.5 mol/L of HNO_3, HCl and H_2SO_4 solutions at 80°C, for 2 h with a S/L ratio of 20 %wt/vol. The best extractions and overall recovery yields for Ce and La were obtained with HCl and H_2SO_4 (72-80 % and 73-82 %, respectively).

The zeolites were used as sorbent material for CO_2 separation from CH_4, in order to simulate the upgrading of biogas to biomethane. The maximum adsorption rate of CO_2 was 0.778 mol CO_2/kg of zeolite at 3 bar, with a resulting CH_4 recovery of 62 % with 97 %vol as purity.

Although the reuse of all the spent FCCCs generated every year worldwide seems to be far from a realistic

goal, the circular economy approach shall be pursued in the oil refining sector that is one of the most polluting [23]. The technical feasibility of the production of the Na-A zeolite was demonstrated, after having recovered Ce and La.

References

[1] J. Wang, X. Huang, D. Cui, L. Wang, Z. Feng, B. Hu, Z. Long, N. Zhao, J. Rare Earth, **35**, 1141-1148 (2017).
[2] J. Wang, Y. Xu, L. Wang, L. Zhao, Q. Wang, D. Cui, Z. Long, X. Huang, J. Environ. Chem. Eng., **5**, 3711-3718 (2017).
[3] S. Ye, Y. Jing, Y. Wang, W. Fei, J. Rare Earth, **35**, 716-722 (2017).
[4] I. Innocenzi, F. Ferella, I. De Michelis, F. Vegliò, J. Ind. Eng. Chem., **24**, 92-97 (2015).
[5] Z. Zhao, Z. Qiu, J. Yang, S. Lu, L. Cao, W. Zhang, Y. Xu, Hydrometallurgy, **167**, 183-188 (2017).
[6] I. De Michelis, A. Olivieri, S. Ubaldini, F. Ferella, F. Beolchini, F. Vegliò, Int. J. Mining Sci. Tech, **23**, 709-715 (2013).
[7] M.K. Jha, A. Kumari, R. Panda, J.R. Kumar, K. Yoo, J.Y. Lee, Hydrometallurgy, **165**, 2-26 (2016).
[8] H. Hubicka, D. Kołodynska, Hydrometallurgy, **62**, 107-113 (2001).
[9] S.R. Dave, H. Kaur, S.K. Menon, React. Funct. Polym., **70**, 692-698 (2010).
[10] M.J. Page, K. Soldenhoff, M.D. Ogden, Hydrometallurgy, **169**, 275-281 (2017).
[11] D.W. Reed, Y. Fujita, D.L. Daubaras, Y. Jiao, V.S. Thompson, Hydrometallurgy, **166**, 34-40 (2016).
[12] F. Ferella, A. Puca, G. Taglieri, L. Rossi, K. Gallucci, J. Clean. Prod., **164**, 1205-1218 (2017).
[13] F. Ferella, F. Cucchiella, I. D'Adamo, K. Gallucci, J. Clean. Prod., **210**, 945-957 (2019a).
[14] M.R. Gonzales, A.M. Pereyra, R. Zerbino, E.I. Basaldella, J. Clean. Prod., **91**, 187-190 (2015).
[15] E.I. Basaldella, J.C. Paladino, M. Solari, G.M. Valle, Appl. Catal. B-Environ., **66**, 186-191 (2006).
[16] X. Liu, L. Li, T. Yang, Z. Yan, J. Porous Mater., **19**, 133-139 (2012).
[17] E.I. Basaldella, R.M. Torres Sánchez, M.S. Conconi, Appl. Clay Sci., **42**, 611-614 (2009).
[18] L. Di Felice, P.U. Foscolo, L.G. Gibilaro, Int. J. Chem. React. Eng. A, **55**, 9 (2011).
[19] F. Ferella, S. Leone, V. Innocenzi, I. De Michelis, G. Taglieri, K. Gallucci, J. Clean, Prod., **230**, 910-926 (2019b).
[20] H.J. Lee, Y.M. Kim, O.S. Kweon, I.J. Kim, J. Eur. Ceram. Soc., **27**, 561-564 (2007).
[21] J. De C. Izidoro, D.A. Fungaro, J.E. Abbott, S. Wang, Fuel, **103**, 827-834 (2013).
[22] M. Mofarahi, F. Gholipour, Micropor. Mesopor. Mat., **200**, 1-10 (2014).
[23] F. Ferella, I. D'Adamo, S. Leone, V. Innocenzi, I. De Michelis, F. Vegliò, Sustainability, **11**, 113 (2019).